fire

MDPI

Article

Upland and Riparian Surface Soil Processes in an Urban Creek with Native and Non-Native Vegetation after Fire

Alicia M. Kinoshita *, Rey Becerra, Marta Miletić and Natalie Mladenov

Department of Civil, Construction and Environmental Engineering, San Diego State University, San Diego, CA 92108, USA; rbecerra3735@sdsu.edu (R.B.); mmiletic@sdsu.edu (M.M.); nmladenov@sdsu.edu (N.M.)

* Correspondence: akinoshita@sdsu.edu; Tel.: +1-619-594-1330

Abstract: Wildfires can pose environmental challenges in urban watersheds by altering the physical and chemical properties of soil. Further, invasive plant species in urban riparian systems may exacerbate changes in geomorphological and soil processes after fires. This research focuses on the 2018 Del Cerro fire, which burned upland and riparian areas surrounding Alvarado Creek, a tributary to the San Diego River in California. The study site has dense and highly flammable non-native vegetation cover (primarily *Arundo donax*) localized in the stream banks and has primarily native vegetation on the hillslopes. We estimated the post-fire organic matter and particle distributions for six time points during water years 2019 and 2020 at two soil depths, 0–15 cm and 15–30 cm, in upland and riparian areas. We observed some of the largest decreases in organic matter and particle-size distribution after the first post-fire rainfall event and a general return to initial conditions over time. Seasonal soil patterns were related to rainfall and variability in vegetation distribution. The riparian soils had higher variability in organic matter content and particle-size distributions, which was attributed to the presence of *Arundo donax*. The particle-size distributions were different between upland and riparian soils, where the riparian soils were more poorly graded. Overall, the greatest change occurred in the medium sands, while the fine sands appeared to be impacted the longest, which is a result of decreased vegetation that stabilized the soils. This research provides a better understanding of upland and riparian soil processes in an urban and Mediterranean system that was disturbed by non-native vegetation and fire.

Keywords: hydrophobic soil; post-fire; riparian; root–soil interaction

Citation: Kinoshita, A.M.; Becerra, R.; Miletić, M.; Mladenov, N. Upland and Riparian Surface Soil Processes in an Urban Creek with Native and Non-Native Vegetation after Fire. *Fire* **2022**, *5*, 32. https://doi.org/10.3390/fire5020032

Academic Editor: Grant Williamson

Received: 30 January 2022
Accepted: 23 February 2022
Published: 26 February 2022

1. Introduction

Wildfires are increasing in frequency and magnitude under a warming climate, impacting natural resources, infrastructure, and millions of people every year [1]. Simultaneously, human encroachment into fire-prone areas has increased the potential for ignition, as well as risks and damages to human communities, and consequently costs to society [2]. In particular, the number of fires under 5 km^2 in the urban riparian environment has also increased in southern California since 2002 [3]. Landscape conversion due to the expansion of the human population and establishments in southern California (United States) has fragmented chaparral ecosystems and intensified the Wildland–Urban Interface (WUI), leading to the potential for fire ignition [4,5]. Urbanization contributes to larger dry weather baseflow due to impermeable land cover ("urban drool"), which alters native riparian vegetation density and community structure [6]. Higher nutrient loads and more frequent flash floods encourage infestations and the rapid settlement of opportunistic and alien vegetation species [7–10]. The high density of non-native vegetation biomass and plant infestations can alter riparian hydrological and geomorphological regimes [11–13] and fire patterns [7,8,11].

Disturbances such as drought, human ignition sources, vegetation type conversion, and fuel accumulation have transformed many WUI riparian areas into corridors for

fire movement [8,14,15], which has environmental and economic implications. However, research is needed to improve the prediction of sediment transport in urban Mediterranean systems, where geomorphic and hydrologic regimes are heavily altered by human activities, which, in return, has consequences for fire regimes and frequency [8,11,13]. The feedback from anthropogenic disturbance to fire regime changes result in altered soil processes and the potential to impact drinking water and recreational bodies of water [6,16].

In Mediterranean systems, the cyclical nature of sediment supply and storage is dependent on the vegetation density and type, which acts as dams that store sediment prior to fire [17]. After a fire, organic matter (OM) from vegetation condenses in the soil horizon and forms a water-repellent layer, which can vary with respect to burn severity [18,19]. This hydrophobic layer facilitates sediment mobilization during precipitation and contributes to landscape development [20]. Loss of vegetation, reduced infiltration [21], soil cohesion [22], and soil water repellency [23] alter surface runoff and erosion potential [24–26] as well as suspended sediment discharge and sedimentation [27,28]. These processes are influenced by characteristics such as slope, surface roughness, vegetation, and rainfall intensity [29]. Elevated quantities of sediment, coupled with flashier post-fire hydrological regimes, often induce significant geomorphic responses such as aggradation, incision, bank widening, channel narrowing, and braiding (i.e., [30,31]). The natural mitigation of these processes is the reestablishment of native vegetation cover [32].

Previous studies have observed the different impacts of fire between upland and riparian regions [14,33]. In Mediterranean climates, chaparral-vegetated hillslopes transition into riparian areas where the canopy and soil moisture are different [33,34]. After a fire, native riparian species often exhibit rapid recovery in biomass in comparison to upland chaparral, generally reinstating the geomorphic stability of the channel area [33]. However, non-native vegetation disrupts traditional hydrologic and geomorphic processes. In contrast to areas with native vegetation, watersheds that are overgrown with non-native vegetation can contribute continuous fuel for a fire, playing a key role in the invasive grass–fire cycle [8,13,15]. Originally introduced to California for erosion control and building materials [8], *Arundo donax* is now ubiquitous across all major coastal watersheds in southern California [13]. *Arundo donax* thrives in urban channels and waterways, growing in monotypic stands that are both highly prone to fire [8,13] and facilitate lateral bank erosion through undercutting and collapse [11]. Furthermore, *Arundo donax* typically recovers more quickly from fire than native vegetation [35].

While there are studies that investigate the effects of fire on the geomorphology of riparian areas with invasive plants (i.e., [11,12]), there is little research that compares upland and riparian soil characteristics under these conditions. Similarly, there are studies that investigate the physical and chemical changes of soil by fire under typical Mediterranean ecosystem conditions [36–38], but do not consider the alterations of soil processes driven by human influence. Thus, this research focuses on the 2018 Del Cerro fire, which burned upland and riparian areas surrounding Alvarado Creek, an urban tributary in San Diego, California to understand surface soil processes. We estimate the post-fire organic matter and soil distributions for six time points during water years 2019 and 2020 at two soil depths in upland (primarily native vegetation) and riparian (primarily non-native vegetation) areas.

2. Materials and Methods

2.1. Study Area

Alvarado Creek is one of the nine tributaries encompassed within the San Diego River watershed located in San Diego, California (Figure 1). The climate in San Diego is Mediterranean with consistent temperatures throughout the year. Precipitation mainly occurs during late November through March but is variable from year to year. The Alvarado Creek watershed consists of developed urban land comprised of residential, industrial, and institutional land uses. Sources of surface runoff to the watershed include Lake Murray, urban runoff, and nearby steep areas through concrete channels and culverts. The study reach consisted of native plants such as *Artemisia californica* and *Muhlenbergia rigens* in the

uplands and dense invasive plant species such as *Arundo donax* and *Washingtonia* spp. in the riparian areas [12]. Prior to the fire, non-native riparian vegetation constricted the stream channel and contributed to flooding during precipitation events.

Figure 1. The study area, Alvarado Creek, is located in San Diego, California (**left image**). A Google Earth Image of the study reach (in blue) in Alvarado Creek (**right image**). The arrows indicate the direction of streamflow. The orange line denotes the Del Cerro fire perimeter. The solid white line is the approximate location of a transect established in the study site where soil samples were collected. The pebble count method to estimate stream-bed material was conducted approximately along the dotted line, where the transect intersects the study reach.

In June of 2018, the Del Cerro fire consumed 38 acres of vegetation in the Alvarado Creek watershed (Figure 1). The soil burn severity was higher in the riparian area compared to the low to moderate soil burn severity in the uplands [3,12]. Following the fire, *Arundo donax* thrived and matured rapidly after several months, while the native riparian vegetation had a slower regrowth [12].

2.2. Precipitation

Daily precipitation data were acquired from MesoWest [39]. Station DW3640 is part of the Citizen Weather Program in San Diego, California, which is near Alvarado Creek. Station DW3640 was assumed to be representative of Alvarado Creek due to its proximity (less than 2 km away) and minimal elevation difference. We identified storm events that had total rainfall greater than 10 mm following the fire and estimated the maximum 15-min rainfall intensity (I15) for each storm event between October 2018 to October 2020. The I15 for each storm was associated with the National Oceanic and Atmospheric Association Atlas (NOAA) ATLAS 14-point precipitation frequency to estimate the magnitude of precipitation events.

2.3. Soil Sampling

Soil samples were obtained from two locations along a previously established transect [12,40]. The upland location was located where chaparral vegetation was burned and the riparian was located adjacent to the stream, where *Arundo donax* was present (Figure 1). Between 26 October 2018 and 22 October 2020, soils were sampled at an upper (0–15 cm) and lower (15–30 cm) depth at each location (Table 1). Three samples were taken at each location to consider inherent variability. Soils collected on 26 October 2020 represent conditions immediately after the fire, as precipitation is the main driver of geomorphic and hydrologic change after the fire. Thus, measurements were generally before and after the wet seasons or, when feasible, after notable rainfall events.

Table 1. Sampling dates and location descriptions.

Date (mm/dd/yyyy)	Description	
	Riparian	**Upland**
10/26/2018	Burned palm trees near the channel	No vegetation
2/15/2019	*Arundo donax* resprouting	No vegetation
9/21/2019	*Arundo donax* regrowth	Sparse regrowth
2/1/2020	Established *Arundo donax* monocultures	Moderate regrowth
6/30/2020	Abundant regrowth	Abundant regrowth
10/22/2020	Abundant regrowth	Abundant regrowth

2.4. Loss on Ignition

Soil organic matter (SOM) content was measured as a loss on ignition (LOI) for two samples per location and depth and in triplicate (twelve total per location). Samples were hand-homogenized, sieved to <2 mm, placed in a weighing dish, and dried overnight (>16 h) in a Yamato DX400 drying oven at 105 °C. Subsequently, 10 g of dried samples were separated into replicates that were placed in aluminum weighing boats of known mass and introduced into a Lindberg Blue Muffle Furnace at 550 °C for four hours [41]. The organic matter (OM) was calculated as:

$$OM = \sum \frac{W_{dry} - W_{after\ ignition}}{W_{dry}} * 100 \quad (1)$$

where W_{dry} is the weight of the dry soil and $W_{after\ ignition}$ is the weight of soil after ignition.

Student's unpaired two-tailed *t*-tests were used to evaluate the statistical significance between sites and depths. If the *p*-value was less than the significance level of 0.05, we rejected the null hypotheses that the means were equal and the difference was statistically significant.

2.5. Soil Classification

We used the ASTM D6913-17 standard test methods for particle-size distribution of soils using sieve analysis [42] and ASTM D4318-17 standard test methods for liquid limit, plastic limit, and plasticity index of soils [43] to classify soil samples for each location and depth in duplicate. Visible foreign objects such as fabrics, shells, or metals were removed from the samples. Soils were pre-treated by removing the organic matter contents and separating the soil particles [44,45]. The samples were submerged into large beakers with distilled water and stirred vigorously. Fine particles were allowed to settle for 10 min, then suspended organic contents were removed using fine strainers. This process was repeated three times to increase the removal of organics. While this process did not completely remove the presence of organics in soil samples, it was minimized to limit the impact on the sieve analysis.

For each location and depth, the soil retained in each sieve was measured. We also expressed the results of the sieve analysis in terms of the percentage of the total weight of soil that passed through different sieves, presented by semi-logarithmic plots of the particle diameters in log scale and the corresponding percent finer. The percentages of gravel, sand, silt, and clay-size particles that were present in the soil were obtained from the particle-size distribution curve. According to the Unified Soil Classification System (USCS) [46], the sizes for gravel, sand, and fines (silt and clay) are defined as >4.75 mm, 4.75 to 0.075 mm, and <0.075 mm, respectively. Fine, medium, and coarse sand are defined as 0.075 to 0.425 mm, 0.425 to 2.0 mm, and 2.0 to 4.75 mm, respectively. To quantify the change from October 2018 with respect to each sampling date, a two-sample Kolmogorov–Smirnov (KS) test was used to compare the distributions. The KS null hypothesis is that distributions were the same at $\alpha = 0.05$ [47].

2.6. Stream-Bed Material

The pebble count method [48] is a quick and simple technique to characterize streambed materials that can be utilized to estimate if disturbances are introducing fine sediments into streams [49]. Following the Wolman (1954) method, we sampled the intermediate axis of 100 pebbles picked from the bed of the stream channel. Using this sample, we established a frequency distribution and estimated the D_{50}, which represents the median substrate size, of which 50% of the samples are equal to or smaller than. We utilized this method to monitor the stream-bed material within the channel that intersects the location of the soils sampled (Figure 1). Samples were available for October 2018, March 2019, and September 2020. We also sampled a reference reach that was unburned and approximately 1.5 km upstream; samples were available for February 2018 and June 2020.

3. Results

3.1. Precipitation

Sixteen storm events occurred over the study period following the Del Cerro fire (Table 2). The average total rainfall was 38 mm, the average I15 was 3.7 mm/hr, and the maximum recurrence interval (RI) was 2–5 years. There were no significant storms immediately following the fire in June 2018, thus soil sampling on October 28, 2018 was considered a baseline or representative of burned soil conditions. Between the first two samples, 26 October 2018 to 15 February 2019, there were eight storm events (Table 2, #1–8) with a total of 309 mm of rainfall, and the largest I15 was 8.4 mm/hr, which was a 2-year event. There was a small storm (#9) between the February 2019 and September 2019 samples (<1 year, Table 2). There were four storm events (Table 2, #10–13) between the September 2019 and February 2020 sampling, with a total rainfall of 199 mm, and the largest I15 was 7.4 mm/hr (RI < 1 year). There were three storm events (Table 2, #14–16) between February 2020 to June 2020 samples, with a total rainfall of 217 mm and the largest I15 was 7.6 mm/hr. Finally, there were no storms between the June and October samples collected in 2020.

Table 2. Precipitation, maximum 15-min intensity (I15), recurrence interval, and total rainfall for significant events during the study period. Soil data were collected in between the dates above and below each horizontal line.

Event #	Date (mm/dd/yyyy)	I15 (mm/hr)	RI (yr)	Total (mm)
1	11/29/2018	3.3	<1	25.1
2	12/5/2018	8.4	2	92.2
3	1/5/2019	1.3	<1	14.2
4	1/12/2019	1.8	<1	11.9
5	1/14/2019	1.3	<1	32.3
6	1/31/2019	3.8	<1	19.1
7	2/2/2019	2.8	<1	50.0
8	2/13/2019	1.3	<1	64.5
9	3/11/2019	1.0	<1	12.2
10	11/19/2019	7.4	<1	32.0
11	11/27/2019	4.8	<1	50.8
12	12/4/2019	4.6	<1	44.7
13	12/23/2019	4.3	<1	71.1
14	3/9/2020	1.3	<1	15.2
15	3/12/2020	3.6	<1	51.3
16	4/6/2020	7.6	2–5	150.4

3.2. Soil Organic Matter

We evaluated the organic matter present in the upland and riparian sites at two depths (Figure 2). The average upland and riparian organic matter ranged from 6.04 to 6.56%. Across all the samples available, the average organic matter between the upland and

riparian soils at both depths was statistically different. The organic matter in the upland upper and lower soils was statistically different but statistically similar at both depths in the riparian soils.

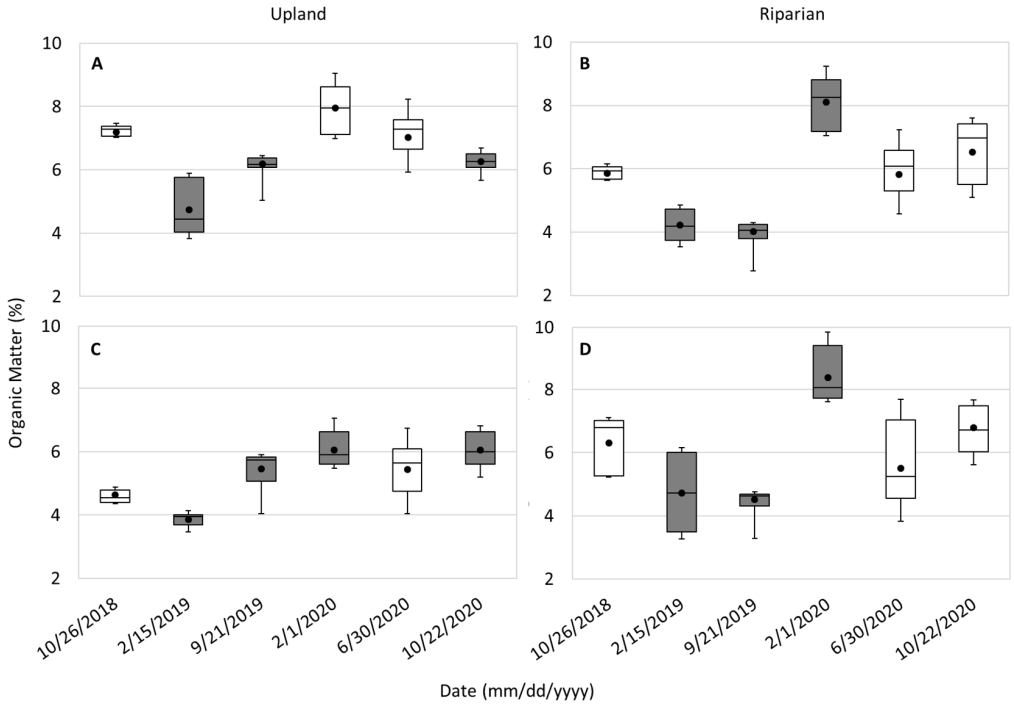

Figure 2. Organic matter box and whisker plots for the upland upper (**A**) and lower (**C**) and riparian upper (**B**) and lower (**D**) soil depths. Dates that are different from 26 October 2018 and statistically significant are shaded.

Soils were collected after the fire (26 October 2018) and represent the immediate post-fire conditions. The observed decrease in SOM in the uplands and riparian at both soil depths between October 2018 to February 2019 was statistically significant (Figure 2). In the second year, the largest change in organic matter content observed across both sites and depths was in February 2020. The smallest change in SOM for both depths was observed on 15 February 2019 for upland areas and on 21 September 2019 for riparian areas.

In the upland areas, the organic matter contents measured in the upper and lower depths were statistically different for all sampled dates except 22 October 2020. Meanwhile, the SOM in both depths was similar for all dates except 21 September 2019 in the riparian. Over the study period, the upland upper depth SOM was statistically similar in February and June of 2020 but different in October 2020. However, the organic matter observed in the riparian upper and bottom layers was statistically different for the three dates following the initial conditions in October 2018 and returned to baseline conditions in June and October 2020.

3.3. Initial Soil Classification

We estimated the particle-size distribution of the soil collected from the upper and lower soil depths of the upland and riparian areas (Figure 3). Due to COVID-19 safety protocols, access to laboratories was limited in 2020 and, thus, sieve analysis was limited and not performed for the upland samples in October 2020 and the riparian samples in June 2020 and October 2020. Before the first rainfall event, the percentage of the fine particles in the upland soils was 18%. The liquid limit of fine particles was 41, and the plasticity index was 5; thus, the soil was classified as silty sand [46]. In the riparian area, the percentage of fine particles was 13%. The liquid limit and plasticity index were 45 and 2, respectively; thus, the soil was also classified as silty sand [46]. In some cases, the percentage of fine

particles decreased below 12%, indicating that soil classifications were not silty sand after the first storm season (described further below).

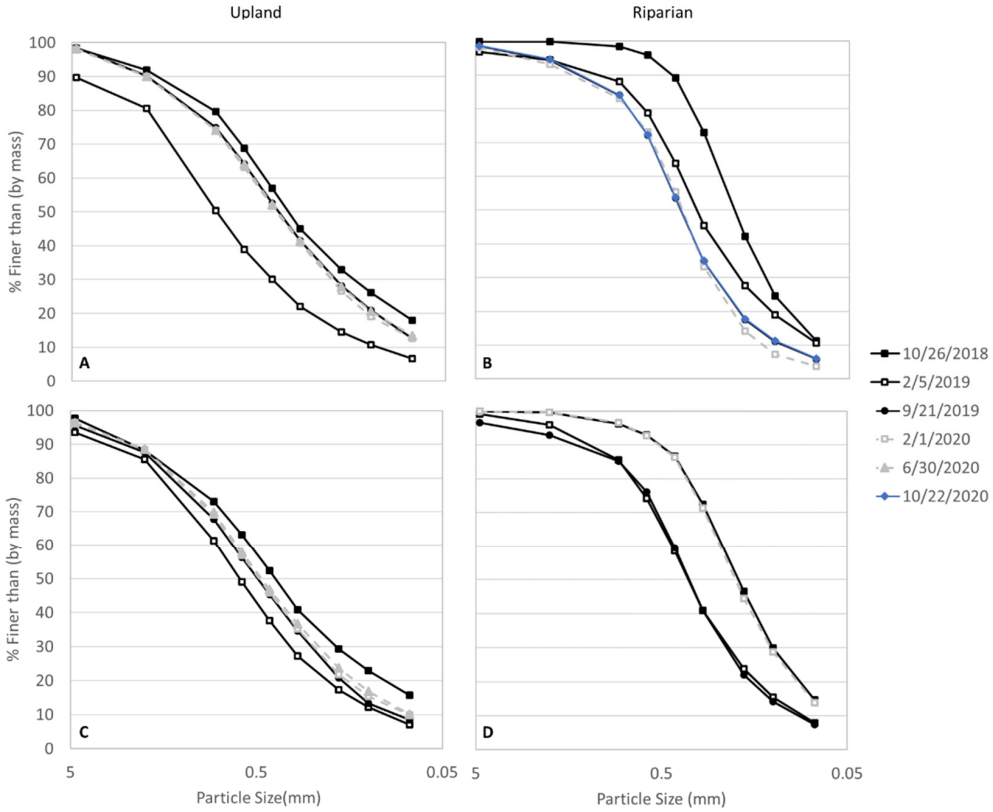

Figure 3. Particle-size distribution for (**A**) upland and (**B**) riparian upper soil depths and (**C**) upland and (**D**) riparian lower soil depths.

3.4. Particle-Size Distribution

Generally, in the uplands, the percent finer by mass was more well-graded and distributed across all sieve sizes (0.075 to 4.75 mm), where larger percent finer occurred in the larger sieve openings and decreased with smaller sieve sizes (Figure 3A,C). Both locations generally contained high frequencies of medium and coarse sand particles (0.425 to 4.75 mm). However, the riparian soils were more poorly graded compared to the uplands (Figure 3B,D), especially for medium and coarse grain sizes for both layers in October 2018 and the bottom layer on 30 June 2020.

In the upland and riparian top and bottom layers, there was a noticeable decrease in the percent finer distributions between October 2018 to February 2019 (Figure 3). The largest difference was observed in the medium sands, 0.425 mm. The upper and lower soils in the uplands had an initial shift or decrease in the frequency of percent finer than by mass across all sand grades during the first wet season (Figure 3A,C). By the start of the second wet season, observed sediment sizes in the upper upland soils nearly returned to initial conditions, stabilizing in the following soil samples (Figure 3A). In the lower upland soils, the distributions remain similar across all sampling dates (Figure 3C). However, the soil type after the first post-fire storm season transitioned to poorly graded sand with silt (fines were between 5–12%). The fine sand in both upper and lower layers did not increase to initial conditions (Figure 3A,C).

The upper riparian soils generally were poorly graded sand with silt (fines were generally between 5–12%) for all samples. Similar to the uplands, there was an initial shift that occurred during the first wet season in the upper and lower riparian soils (Figure 3B,D). However, in the upper riparian soils, the particle-size distribution continued to decrease in September 2019, February 2020, and October 2020 (Figure 3B). In the lower riparian

soils, the February 2019 and September 2019 distributions were similar and transitioned to poorly graded sand with silt compared to the silty sand classified in October 2018. Silty sand is noted in February 2020 as there was an increase to the initial conditions (Figure 3D).

The KS null hypotheses that the distributions were the same for all dates compared to the October 2018 distributions for each soil layer and location, were accepted, thus, all shifts observed were not significant.

We also investigated the mass retained from the sieve analysis in general; the percent of mass retained in the upland soils was consistent across the clay and fine and medium sand (<0.075 to 0.425 mm; Figure 4A,C), while the percentage of coarse (4.75 mm) mass retained was lower. There was a tendency towards medium mass retained (0.85 mm) in both depths in the uplands. The upland upper soil had a general increase in mass retention in diameters 0.6 to 4.75 mm and a decrease in diameters <0.075 to 0.425 mm between October 2018 and February 2019 (Figure 4A). In the upper soil depth of the uplands, there was over a 530% increase in coarse mass retained from October 2018 to February 2019 and a general return to initial conditions over the following dates. In the upper soils, there was also a 25% and 50% decrease in medium and fine sands, respectively, from October 2018 to February 2019 and a return to initial conditions over the following dates. In the upland lower depth, there was over a 170% and 92% increase in the coarse mass retained from October 2018 to February 2019 and September 2019, respectively, and ~30% decrease in the fine sands for several samples following October 2018. Silt and clay in the upland upper and lower depths also had a significant decrease in the first storm season and remained below initial conditions for the remainder of the samples.

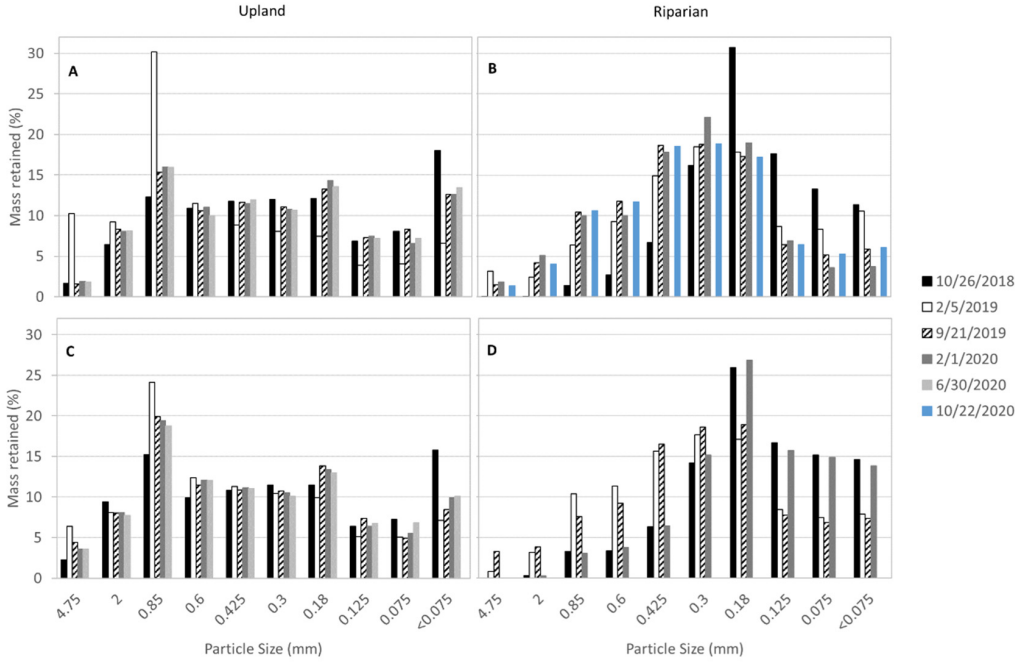

Figure 4. Percent of soil mass retained per sieve size for the (**A**) upland and (**B**) riparian upper soil depths and (**C**) upland and (**D**) riparian lower soil depths.

The upper riparian generally followed a more normal distribution of mass retained (Figure 4B), where there were higher percentages of mass retained in the fine sands (0.18 to 0.425 mm). The riparian upper soil had a general increase in mass retention in diameters > 0.30 mm and a decrease in sizes < 0.18 mm (Figure 4B). In the upper riparian, the coarse sand greatly increased from 0.02% in October 2018 to 1.44 to 3.19% and medium sand increased from 6.67% to 14.90 to 18.70% in the three subsequent samples. The fine sand and silt and clay had a continued loss and lower mass retention in all samples after October 2018. The lower riparian showed similar patterns as the upper soil (increase

in medium and coarse sands and decrease in fine sand and clay and silt), however, the mass retained across most of the diameters returned to initial conditions in February 2020.

3.5. Stream-Bed Material

We sampled the stream-bed material adjacent to the upland and riparian soil. The D_{50} after the fire and prior to the storm season was 115 mm. After the first storm season, the D_{50} was 55 mm in March 2019 and returned to 102 mm in September 2020. Meanwhile, the reference reach maintained a D_{50} of 100 and 105 mm for February 2018 and June 2020.

4. Discussion

4.1. Organic Matter

Immediately after the fire, the organic matter in the uplands was higher in the upper soils than in deeper soils compared to the riparian area, where no significant differences were observed (Figure 2). This could be indicative of the buildup of dense and mature chaparral stands in the uplands that accumulated on the surface prior to the fire [50]. This was in contrast to the riparian area, which may be influenced by the stream and coarser sand material. Charred vegetation was deposited on the soil surface and subsurface following the fire, which was observed in the October 2018 analysis (Figure 2A). Oguntunde et al. [37] showed that the combination of fire-formed charcoal and charred residue can change the soil physical properties and, thus, affecting post-fire soil processes. Specifically, saturated hydraulic conductivity, total porosity, bulk density, sand fraction, and infiltration rates of soils were altered and attributed to changes in soil structure [37]. Following eight rainfall events in the first post-fire storm season, the February 2019 upland and riparian upper and lower soils had a statistically significant decrease in organic matter, which was attributed to the significant loss of unprotected soil due to fire. In the uplands, the decrease in organic matter between October 2018 and February 2019 was the largest observed. Vegetation mortality during or after a fire can contribute to the washout of organic compounds by throughfall. Additionally, fires can alter soil properties that may induce water repellency and reduce the amount of time water is retained in soils, which has implications for dissolved organic carbon mobilization [38,40,51]. On subsequent dates, the upland soils had an increasing organic matter trend, which likely followed the steady regrowth and deposition of plant matter that is often observed in the post-fire recovery of chaparral vegetation [50,52]. Further, we observed that the organic matter in the lower upland soils was relatively stable compared to the upper uplands and riparian soils (Figure 2C).

While the vegetation biomass of *Arundo donax* was greater than native chaparral in the uplands immediately after the fire, the uplands generally had a higher organic matter content. The riparian area was dominated by *Arundo donax*, which likely impacted the difference in the observed organic matter patterns. While the upland soils appeared to have a more stable increase, there was more variability observed in the riparian organic matter. Both locations were sensitive to rainfall, which was noticeable in February 2020, and may be due to decay of the deposited plant material and incorporation into the SOM pool under wetter conditions. Similar to the uplands, there was a significant decrease between October 2018 and February 2019. However, there was a second and larger decrease in organic matter in the riparian soils between February 2020 and June 2020, which is attributed to the hydrologic and vegetation dynamics. The higher variability in the riparian soils may be an indicator of the sensitivity of invasive vegetation to available water. Grasses are particularly sensitive to rainfall due to shallow roots [53], which may contribute to the rapid growth and senescence of *Arundo donax* and, consequently, SOM. Additionally, *Arundo donax* has extremely dense root structures mostly within a depth of 30 cm and the root diameter can range between 1.0 mm to 20.0 mm [11], which can contribute to more mobile soils that can dislodge the organic horizon. This contrasts the deep penetrating or shallow wide-spreading or branching fibrous roots of some southern Californian chaparral [54]. The difference between the root structures may alter the presence of organic matter. Further, we followed the standard LOI technique to separate sediment and residues larger than

2 mm prior to estimating the organic content, which could have contributed to overlooking roots larger than 4.25 mm.

4.2. Sediment Transport Patterns

There was an overall decrease in the particle size across all soils (Figure 3). The greatest change occurred in the medium sands, while the fine sands appeared to be impacted the longest (Figure 3). We observed the release of smaller sediment and coarsening of the soil (Figure 4), which is a natural geomorphic response to stabilize the landscape with larger grain sizes [55–57]. This also corroborates field observations by Mathews et al. [12], who noted that fine sediments were removed from the uplands, where rainfall intensity surpassed the saturated hydraulic conductivity of the finest layer of the hillslope. Severely heating soils can also alter the particle-size distribution and result in coarser textures due to an increase in silt fraction [36]. Coarsening patterns also corresponded to our observations in the adjacent channel, where there was a removal of the fines, leaving coarser particles in the streambed, and suggesting the role of the fire.

In the uplands, the first post-fire storm season had the largest shift (Figure 3A), which was likely due to the loss of vegetation. Vegetation acts as dams that retain sediment; when vegetation is disturbed or removed by fire, sediment is released to the stream margins due to gravity through a mechanism known as dry ravel [17]. Further, during rain events, unprotected soils are more mobile and sediment is more susceptible to transport [27]. Finer sediment leaves the soil profile, increasing the coarser particles after the first wet season [57], which we observed in this study (Figure 4). Decreased vegetation cover followed by rainfall was the primary driver of fine sediment removal; expedited and elevated quantities of fine sediment transport were also noted by studies such as Syvitski et al. [30] and Chin et al. [31].

The natural mitigation of fire-driven erosion and the resultant geomorphic change is the reestablishment of native vegetation cover [32]. In Alvarado Creek, very little vegetation recovery occurred on the upland hillslope between June 2018 to the end of March 2019 and corresponded with the largest measured geomorphic response following the first post-fire storm event, which progressively decreased thereafter [12]. This is common in systems with chaparral species, which have deep root systems that can stabilize soil mass and reduce surface soil movement [54]. Thus, the immediate release of sediment, coupled with an armored hillslope due to deep chaparral root systems [54] and large clast grain structure [57], can result in a smaller sediment discharge, despite the flushing of soils by rain events. In Alvarado Creek, the removal of the topsoil and ash deposits after the first storm event was documented in the field by Mathews et al. [12], leaving only the charred layer that was beneath the initial horizon and a coarser grain size distribution. The removal of the smaller grain sizes likely occurred by erosional mechanisms such as rain splash, overland sheet flow, or thin debris flows [58,59], resulting in a coarsening of soils. In our study area, the higher frequency of larger grain sizes may have contributed to the geomorphic stability of the landscape after the first storm event by increasing the resilience to shear stress that could initiate particle transport during future precipitation events [55,56]. This is due to the low burn severity observed in the uplands, leaving the native chaparral roots mostly intact, and fortifying the structural integrity of the hillslope from hydraulic events [57].

The sediment processes in the riparian zone were more dynamic. In the floodplains of southern California, the high tensile strength and dense root structure of *Arundo donax* can induce bank instability and subsequently bank collapse during severe floods [8,11]. The high variability in soil characteristics and preferential retention of coarse and medium sands in the riparian soils (Figure 3B,D) were attributed to the fast vegetation regrowth dominated by monocultures of *Arundo donax* and resultant geomorphic instability [12]. We hypothesize that *Arundo donax* outcompeted native vegetation and facilitated a coarsening of sediment and a decrease in fine sand, silt, and clay particles. The roughness and rhizome root structures imposed by *Arundo donax* infestations decreased hydraulic velocities and

flooding, which contributed to preferential sediment deposition, armoring of the channel, and lateral bank movement [60,61]. The aggradation of the floodplain, channel incision, and obliteration of step-pool morphology observed by Mathews et al. [12] resulted in a sustained topographic change in the riparian area surrounding Alvarado Creek and supports our observations.

5. Conclusions

This study investigated soil organic matter and particle-size distribution in Alvarado Creek, an urban Mediterranean system, to understand the post-fire soil patterns in upland hillslopes with native vegetation and riparian areas with non-native vegetation after fire. In the upland hillslopes, with predominantly native chaparral, fine grains comprised the main sediment transported. This research builds upon our knowledge of how the presence of *Arundo donax* in urban Mediterranean systems can disrupt soil regimes. The presence of monocultures of *Arundo donax* and rapid regrowth after fire had a significant impact on the retention of coarse sediment, which armored channels to decrease faster flows. This has implications for river restoration activities that are intended to manage non-native vegetation and alleviate fire hazards and channel capacity to reduce flooding. Further, the presence of *Arundo donax* in stream channels and riparian areas creates a more dynamic system and imposes higher risks to future fire events, which can further exacerbate geomorphology and can create hazardous conditions.

Author Contributions: Conceptualization, A.M.K. and R.B.; methodology, A.M.K., R.B., M.M., N.M.; formal analysis, R.B., A.M.K.; investigation, R.B., A.M.K.; resources, A.M.K.; writing—original draft preparation, R.B., A.M.K.; writing—original draft and review and editing, R.B., A.M.K., M.M., N.M.; visualization, A.M.K.; supervision, A.M.K.; project administration, A.M.K., M.M.; funding acquisition, A.M.K. All authors have read and agreed to the published version of the manuscript.

Funding: This material is based upon work supported by the National Science Foundation CAREER Program under Grant No. (1848577); the California State University (CSU) Council on Ocean Affairs, Science & Technology (COAST) Rapid Response Funding Program Award #COAST-RR-2017-04, the Office of Naval Research award for Advancing Navy STEM Workforce through Education and Research (ANSWER) #N00014-18-1-2365; and San Diego River Conservancy under grant number SDRG-P1-18-15. The APC was funded by MDPI.

Institutional Review Board Statement: Not applicable.

Informed Consent Statement: Not applicable.

Data Availability Statement: Data is contained within the article or upon request.

Acknowledgments: The authors would like to acknowledge Y. Wu and J. Valdes for providing lab space and materials to conduct the experiments described in this paper. We also thank Q. Alkin, L. Mathews, D. Hunt, B. Wilder for their help in the field. Additionally, we thank T. Eckermann and G. Goncalves-Santana for their contributions.

Conflicts of Interest: The authors declare no conflict of interest. The funders had no role in the design of the study; in the collection, analyses, or interpretation of data; in the writing of the manuscript, or in the decision to publish the results.

References

1. Bowman, D.M.J.S.; Balch, J.K.; Artaxo, P.; Bond, W.J.; Carlson, J.M.; Cochrane, M.A.; D'Antonio, C.M.; DeFries, R.S.; Doyle, J.C.; Harrison, S.P.; et al. Fire in the Earth System. *Science* **2009**, *324*, 481–484. [CrossRef] [PubMed]
2. Gorte, R. The Rising Cost of Wildfire Protection. *Headwaters Econ.* **2013**, *19*. Available online: https://www.baileyhealthyforests.org/wp-content/uploads/2013/12/fire-costs-background-report.pdf (accessed on 19 January 2022).
3. Mathews, L.; Kinoshita, A. Urban Fire Severity and Vegetation Dynamics in Southern California. *Remote Sens.* **2021**, *13*, 19. [CrossRef]
4. Syphard, A.D.; Radeloff, V.C.; Keeley, J.E.; Hawbaker, T.J.; Clayton, M.K.; Stewart, S.I.; Hammer, R.B. Human influence on California fire regimes. *Ecol. Appl.* **2007**, *17*, 1388–1402. [CrossRef] [PubMed]
5. Syphard, A.D.; Brennan, T.J.; Keeley, J.E. Drivers of chaparral type conversion to herbaceous vegetation in coastal Southern California. *Divers. Distrib.* **2019**, *25*, 90–101. [CrossRef]

6. White, M.D.; Greer, K.A. The effects of watershed urbanization on the stream hydrology and riparian vegetation of Los Peñasquitos Creek, California. *Landsc. Urban Plan.* **2006**, *74*, 125–138. [CrossRef]
7. D'Antonio, C.M. Fire, Plant Invasions, and Global Changes. In *Invasive Species in a Changing World*; Hobbs, R.J., Ed.; Island Press: Covela, CA, USA, 2000; pp. 65–93. ISBN 978-1-59726-337-5.
8. Coffman, G.C.; Ambrose, R.F.; Rundel, P.W. Wildfire promotes dominance of invasive giant reed (Arundo donax) in riparian ecosystems. *Biol. Invasions* **2010**, *12*, 2723–2734. [CrossRef]
9. Godefroid, S.; Koedam, N. Urban plant species patterns are highly driven by density and function of built-up areas. *Landsc. Ecol.* **2007**, *22*, 1227–1239. [CrossRef]
10. Aronson, M.F.; Lepczyk, C.A.; Evans, K.L.; Goddard, M.; Lerman, S.B.; MacIvor, J.S.; Nilon, C.H.; Vargo, T. Biodiversity in the city: Key challenges for urban green space management. *Front. Ecol. Environ.* **2017**, *15*, 189–196. [CrossRef]
11. Stover, J.E.; Keller, E.A.; Dudley, T.L.; Langendoen, E.J. Fluvial Geomorphology, Root Distribution, and Tensile Strength of the Invasive Giant Reed, Arundo Donax and Its Role on Stream Bank Stability in the Santa Clara River, Southern California. *Geosciences* **2018**, *8*, 304. [CrossRef]
12. Mathews, L.; Kinoshita, A. Vegetation and Fluvial Geomorphology Dynamics after an Urban Fire. *Geosciences* **2020**, *10*, 317. [CrossRef]
13. *California Invasive Plant Council (Cal-IPC) Arundo Donax (Giant Reed): Distribution and Impact Report*. 2011. Available online: https://www.cal-ipc.org/wp-content/uploads/2017/11/Arundo_Distribution_Impact_Report_Cal-IPC_March-2011_small.pdf (accessed on 19 January 2022).
14. Pettit, N.E.; Naiman, R.J. Fire in the Riparian Zone: Characteristics and Ecological Consequences. *Ecosystems* **2007**, *10*, 673–687. [CrossRef]
15. Cushman, J.H.; Gaffney, K.A. Community-level consequences of invasion: Impacts of exotic clonal plants on riparian vegetation. *Biol. Invasions* **2010**, *12*, 2765–2776. [CrossRef]
16. Stein, E.D.; Brown, J.S.; Hogue, T.S.; Burke, M.P.; Kinoshita, A. Stormwater contaminant loading following southern California wildfires. *Environ. Toxicol. Chem.* **2012**, *31*, 2625–2638. [CrossRef] [PubMed]
17. Lamb, M.P.; Scheingross, J.S.; Amidon, W.H.; Swanson, E.; Limaye, A. A model for fire-induced sediment yield by dry ravel in steep landscapes. *J. Geophys. Res. Earth Surf.* **2011**, *116*. [CrossRef]
18. DeBano, L.F.; Rice, R.M. Water Repellent Soils: Their Implications in Forestry. *J. For.* **1973**, *71*, 220–223. [CrossRef]
19. Lewis, S.A.; Wu, J.Q.; Robichaud, P.R. Assessing burn severity and comparing soil water repellency, Hayman Fire, Colorado. *Hydrol. Process.* **2006**, *20*, 1–16. [CrossRef]
20. DeBano, L.F.; Rice, R.M.; Eugene, C.C. *Soil Heating in Chaparral Fires: Effects on Soil Properties, Plant Nutrients, Erosion, and Runoff*; Res. Paper PSW-RP-145; U.S. Department of Agriculture, Forest Service, Pacific Southwest Forest and Range Experiment Station: Berkeley, CA, USA, 1979; Volume 145, 21p. Available online: https://www.fs.usda.gov/treesearch/pubs/29933 (accessed on 19 January 2022).
21. Moody, J.A.; Shakesby, R.A.; Robichaud, P.R.; Cannon, S.H.; Martin, D.A. Current research issues related to post-wildfire runoff and erosion processes. *Earth-Sci. Rev.* **2013**, *122*, 10–37. [CrossRef]
22. Robichaud, P. Fire effects on infiltration rates after prescribed fire in Northern Rocky Mountain forests, USA. *J. Hydrol.* **2000**, *231–232*, 220–229. [CrossRef]
23. Letey, J. Causes and consequences of fire-induced soil water repellency. *Hydrol. Process.* **2001**, *15*, 2867–2875. [CrossRef]
24. Kraebel, C.J. The La Crescenta Flood. *Am. For.* **1934**, *40*, 286–287.
25. Rulli, M.C.; Rosso, R. Hydrologic response of upland catchments to wildfires. *Adv. Water Resour.* **2007**, *30*, 2072–2086. [CrossRef]
26. Wittenberg, L.; Malkinson, D.; Barzilai, R. The differential response of surface runoff and sediment loss to wildfire events. *CATENA* **2014**, *121*, 241–247. [CrossRef]
27. DeBano, L.F.; Neary, D.G.; Folliott, P.F. *Fire: Its Effect on Soil and Other Ecosystem Resources*; John Wiley & Sons, Inc.: New York, NY, USA, 1998; pp. 71–159. ISBN 978-0-471-16356-5.
28. Florsheim, J.; Keller, E.A.; Best, D.W. Fluvial sediment transport in response to moderate storm flows following chaparral wildfire, Ventura County, southern California. *GSA Bull.* **1991**, *103*, 504–511. [CrossRef]
29. Nyman, P.; Smith, H.G.; Sherwin, C.B.; Langhans, C.; Lane, P.N.; Sheridan, G.J. Predicting sediment delivery from debris flows after wildfire. *Geomorphology* **2015**, *250*, 173–186. [CrossRef]
30. Syvitski, J.P.; Peckham, S.; Hilberman, R.; Mulder, T. Predicting the terrestrial flux of sediment to the global ocean: A planetary perspective. *Sediment. Geol.* **2003**, *162*, 5–24. [CrossRef]
31. Chin, A.; Solverson, A.P.; O'Dowd, A.P.; Florsheim, J.L.; Kinoshita, A.M.; Nourbakhshbeidokhti, S.; Sellers, S.M.; Tyner, L.; Gidley, R. Interacting geomorphic and ecological response of step-pool streams after wildfire. *GSA Bull.* **2019**, *131*, 1480–1500. [CrossRef]
32. Robichaud, P.R.; Lewis, S.A.; Brown, R.E.; Ashmun, L.E. Emergency Post-Fire Rehabilitation Treatment Effects on Burned Area Ecology and Long-Term Restoration. *Fire Ecol.* **2009**, *5*, 115–128. [CrossRef]
33. Dwire, K.A.; Kauffman, J. Fire and riparian ecosystems in landscapes of the western USA. *For. Ecol. Manag.* **2003**, *178*, 61–74. [CrossRef]
34. Verkaik, I.; Rieradevall, M.; Cooper, S.D.; Melack, J.M.; Dudley, T.L.; Prat, N. Fire as a disturbance in mediterranean climate streams. *Hydrobiologia* **2013**, *719*, 353–382. [CrossRef]

35. Bell, G.P. Ecology and Management of Arundo Donax, and Approaches to Riparian Habitat Restoration in Southern California. Available online: https://ic.arc.losrios.edu/~{}veiszep/05spr2001/stelmok/g26files/attach5.html (accessed on 19 January 2022).
36. Ulery, A.L.; Graham, R.C. Forest Fire Effects on Soil Color and Texture. *Soil Sci. Soc. Am. J.* **1993**, *57*, 135–140. [CrossRef]
37. Oguntunde, P.G.; Abiodun, B.J.; Ajayi, A.E.; van de Giesen, N. Effects of charcoal production on soil physical properties in Ghana. *J. Plant Nutr. Soil Sci.* **2008**, *171*, 591–596. [CrossRef]
38. Certini, G.; Nocentini, C.; Knicker, H.; Arfaioli, P.; Rumpel, C. Wildfire effects on soil organic matter quantity and quality in two fire-prone Mediterranean pine forests. *Geoderma* **2011**, *167–168*, 148–155. [CrossRef]
39. Horel, J.; Splitt, M.; Dunn, L.; Pechmann, J.; White, B.; Ciliberti, C.; Lazarus, S.; Slemmer, J.; Zaff, D.; Burks, J. Mesowest: Cooperative Mesonets in The Western United States. *Bull. Am. Meteorol. Soc.* **2002**, *83*, 211–226. [CrossRef]
40. Alkin, Q.; Kinoshita, A.M. A Case Study of Soil Moisture and Infiltration after an Urban Fire. *Fire* **2020**, *3*, 22. [CrossRef]
41. Wilke, B.-M. Determination of Chemical and Physical Soil Properties. In *Monitoring and Assessing Soil Bioremediation*; Margesin, R., Schinner, F., Eds.; Soil Biology; Springer: Berlin/Heidelberg, Germany, 2005; pp. 47–95. ISBN 978-3-540-28904-3.
42. *ASTM D6913-04*; Standard Test Methods for Particle-Size Distribution (Gradation) of Soils Using Sieve Analysis. 2017. Available online: https://www.astm.org/d6913_d6913m-17.html(accessed on 19 January 2022).
43. *ASTM D4318-17*; Standard Test Methods for Liquid Limit, Plastic Limit, and Plasticity Index of Soils. 2018. Available online: https://www.astm.org/d4318-17e01.html(accessed on 19 January 2022).
44. Day, P.R. Particle fractionation and particle-size analysis. In *Methods of Soil Analysis*; John Wiley & Sons, Ltd.: Hoboken, NJ, USA, 1965; pp. 545–567. ISBN 978-0-89118-203-0. Available online: https://acsess.onlinelibrary.wiley.com/doi/10.2134/agronmonogr9.1.c43 (accessed on 19 January 2022).
45. Kroetsch, D.; Wang, C. Particle size distribution. In *Soil Sampling and Methods of Analysis*; Carter, M.R., Gregorich, E.G., Eds.; Canadian Society of Soil Science; CRC Press: Boca Raton, FL, USA, 2008; pp. 713–725. ISBN 978-0-8493-3586-0.
46. *ASTM D2487*; Standard Practice for Classification of Soils for Engineering Purposes (Unified Soil Classification System). Available online: https://www.astm.org/d2487-17e01.html(accessed on 19 January 2022).
47. Massey, F.J., Jr. The Kolmogorov-Smirnov Test for Goodness of Fit. *J. Am. Stat. Assoc.* **1951**, *46*, 68–78. [CrossRef]
48. Wolman, M.G. A method of sampling coarse river-bed material. *Trans. Am. Geophys. Union* **1954**, *35*, 951–956. [CrossRef]
49. Potyondy, J.P.; Hardy, T. Use of pebble counts to evaluate fine sediment increase in stream channels. *JAWRA J. Am. Water Resour. Assoc.* **1994**, *30*, 509–520. [CrossRef]
50. Rundel, P.W.; Parsons, D.J. Structural Changes in Chamise (Adenostoma fasciculatum) along a Fire-Induced Age Gradient. *Rangel. Ecol. Manag.* **1979**, *32*, 462. [CrossRef]
51. Wei, X.; Hayes, D.J.; Fernandez, I. Fire reduces riverine DOC concentration draining a watershed and alters post-fire DOC recovery patterns. *Environ. Res. Lett.* **2021**, *16*, 024022. [CrossRef]
52. Keeley, J.E.; Keeley, S.C. Post-Fire Regeneration of Southern California Chaparral. *Am. J. Bot.* **1981**, *68*, 524–530. [CrossRef]
53. Prater, M.R.; DeLucia, E.H. Non-native grasses alter evapotranspiration and energy balance in Great Basin sagebrush communities. *Agric. For. Meteorol.* **2006**, *139*, 154–163. [CrossRef]
54. Hellmers, H.; Horton, J.S.; Juhren, G.; O'Keefe, J. Root Systems of Some Chaparral Plants in Southern California. *Ecology* **1955**, *36*, 667–678. [CrossRef]
55. Bridge, J.S. Hydraulic Interpretation of Grain-size Distributions Using a Physical Model for Bedload Transport. *J. Sediment. Res.* **1981**, *51*, 1109–1124. [CrossRef]
56. Lu, N.; Godt, J.W. *Hillslope Hydrology and Stability*; Cambridge University Press: Cambridge, UK, 2013. [CrossRef]
57. Wohlgemuth, P.M. Surface Sediment Transport: A Review of Current Knowledge and a Field Study of Its Spatial and Temporal Distributions in the San Dimas Experimental Forest, California. Master's Thesis, California State University, Northridge, CA, USA, 1986.
58. Gabet, E.J. Post-fire thin debris flows: Sediment transport and numerical modelling. *Earth Surf. Process. Landf.* **2003**, *28*, 1341–1348. [CrossRef]
59. Shakesby, R.; Doerr, S. Wildfire as a hydrological and geomorphological agent. *Earth Sci. Rev.* **2006**, *74*, 269–307. [CrossRef]
60. Spencer, D.F.; Colby, L.; Norris, G.R. An evaluation of flooding risks associated with giant reed (Arundo donax). *J. Freshw. Ecol.* **2013**, *28*, 397–409. [CrossRef]
61. Schoelynck, J.; De Groote, T.; Bal, K.; Vandenbruwaene, W.; Meire, P.; Temmerman, S. Self-organised patchiness and scale-dependent bio-geomorphic feedbacks in aquatic river vegetation. *Ecography* **2011**, *35*, 760–768. [CrossRef]